Study on the arc behavior of laminar plasma arc welding

H. L. Zhao[a], S. Y. Zhang[a], X. L. Yu[a], Y. W. Li[a], J.Y. Miao[a], C. H. Chang[b], Y. L. Chang[a,*]

a. School of Materials Science and Engineering, Shenyang University of Technology, Shenyang 110870, China

b. Liaoning Xinyuan Special Welding Technology Co., Ltd, Shenyang 110011, China

*. Corresponding Author. Tel. :+86-13889129128, Fax:+86-24-25496768.

Email addresses: 273609602@qq.com (H. L. Zhao); 175019133@qq.com (S. Y. Zhang); 577618498@qq.com (X. L. Yu); 1047990174@qq.com (Y. W. Li); 1293802699@qq.com (J.Y. Miao); 2687114369@qq.com (C. H. Chang); zhl08302021@126.com (Y. L. Chang)

Abstract

Laminar non-transfer arc of laminar plasma arc has the characteristics of long jet length, low temperature gradient, and good controllability, and is often used for cutting, spraying, and surface treatment, but rarely for welding due to its lower arc heat. The combined laminar plasma arc, composed of the laminar non-transfer arc and the transfer arc, has better welding penetration, but research on its welding characteristics is still lacking. The arc behavior is studied in this paper to expand its application range. The experimental results show that the laminar plasma arc can be obtained with the proper shielding gas and plasma gas flow. The maximum arc ignition height is mainly determined by non-transfer arc current, while arc shape and arc pressure mainly depend on transfer arc current. The arc pressure sharply decreases with the increase of arc ignition height below 20 mm. Furthermore, potential welding applications and their prospects have been discussed. It was found that the transfer arc plays a crucial role in welding formation, while the non-transfer arc can enhance welding adaptability due to the control of arc ignition height. This heat source is highly suitable for thick plate narrow gap welding and shows promising prospects.

Keywords

Laminar plasma arc welding; Arc shape; Arc pressure; Narrow gap welding; Arc behavior

1 Introduction

Plasma arc is composed of high temperature, high speed, and high energy density plasma gas flow [1]. The arc has three forms: (1) Non-transfer arc. where an arc is generated between the tungsten electrode and the conductive nozzle. (2) Transfer arc. where an arc is generated between the tungsten electrode and the workpiece. (3) Combined arc. where non-transfer arc and transfer arc exist simultaneously.

In the plasma welding torch, plasma gas is introduced between the tungsten electrode and the conductive nozzle, while shielding gas is introduced between the conductive nozzle and the shielding gas nozzle. Both gases used are argon. Gas flow can be generally divided into turbulent flow and laminar flow. Non-transfer arc, in which both the plasma gas and shielding gas are in a turbulent state, is often used in

industrial production [2]. Due to the irregular jumping of the arc root and the shearing effect of high-speed gas flow on the air [3], the arc length is below 20 mm, which makes it difficult to meet the current industrial development requirements. Research shows that [4], when both plasma gas and shielding gas are in laminar flow, the arc length of a non-transfer arc can reach 100 mm. Additionally, the arc exhibits small axial temperature gradients, good stability, and low noise levels. Laminar non-transfer arc has been studied on the relationship between plasma temperature and velocity [5], volt-ampere characteristics [6], and impact characteristics [7]. It has been applied in the fields of metal material cutting [8], material surface treatment [9], spraying [10], and additive manufacturing [11]. The use of laminar non-transfer arc for welding is rare due to its low arc heat and the challenge of quickly penetrating the workpiece. It has been studied to compound it with MIG arc [12], but the weld formation is worse, and the operation is complicated. The study also mentions a welding method that combines laminar non-transfer arc and transfer arc, known as laminar plasma arc welding. However, research on its welding characteristics is still lacking.

Based on the maximum arc ignition height, arc shape parameters, and arc pressure, the welding characteristics of laminar plasma arc have been studied in this paper. This study provides experimental and theoretical support for expanding the welding applications of this technology.

2 Experimental procedure

2.1 Experimental methods

During the experiment, the non-transfer arc is opened first, and then the transfer arc is opened to form a combined arc. The experimental platform used in the study is shown in Fig. 1. Experimental instruments and equipment include: (1) Plasma arc welding machine, with an adjustable transfer arc current of 0-300 A and an adjustable non-transfer arc current of 0-150 A; (2) Plasma arc welding torch with a conductive nozzle aperture of 4 mm and a shielding gas nozzle aperture of 12 mm. A cerium-tungsten electrode, with a diameter of 4 mm and a sharpening angle of 30 degrees, was selected; (3) YRC1000 welding robot; (4) X113 high-speed camera has a frame rate of 2000 frames per second; (5) Small hole arc pressure testing system with a pressure sensor. When the arc passes through the small hole, the arc pressure and arc position are recorded in real time.

2.2 Arc processing

Arc processing is divided into two parts: videos and pictures. The videos are captured by a high-speed camera positioned perpendicular to the arc, while the pictures are made by video editing software combined with picture processing software, such as Adobe Premiere Pro (PR) and Photoshop (PS). First, PR is used to extract pictures from the videos frame by frame and export them at a fixed size. Then, PS is used to standardize the picture parameters, encompassing brightness and threshold [13]. Finally, the processed arc shape figures are obtained, as shown in Fig. 2(c).

Arc projection diameter, arc root diameter, and arc ignition height are expressed by Dp, Dr, and L, respectively. The calculation of scale is obtained using a proportional relation. Based on the outer diameter of the conductive nozzle in the

figure being 53 mm, and the actual diameter being 10 mm, the length relational equation (1) is established. By considering the total area of the picture (141.22×141.22) mm^2 and the total pixels of the picture (250,000), along with the arc pixel *c* in the picture, the actual arc area *d* can be calculated, as shown in equation (2).

$$\frac{a}{b}=\frac{53mm}{10mm}=5.3 \tag{1}$$

$$\frac{c\times(141.22\text{mm}\times141.22mm)}{\frac{250000}{d}}=5.3^2 \tag{2}$$

Where *a* is the length (mm) in the figure, *b* is the actual length (mm), *c* is the arc pixel, and *d* is the actual arc area (mm^2).

3 Results and discussion

3.1 Maximum arc ignition height

Non-transfer arc is generated between the tungsten electrode and the conductive nozzle, which can always be successfully ignited. Therefore, this section mainly focuses on the influencing factors of the maximum ignition height of the transfer arc. The following method was adopted: under a certain parameter, after the non-transfer arc was ignited, the welding torch was continuously raised to try to ignite the transfer arc until it failed, and the data of the maximum arc ignition height under this parameter was recorded.

3.1.1 Shielding/plasma gas flow

The influence of shielding/plasma gas flow on maximum arc ignition height was studied, as shown in Fig. 3. Among them, the fixed transfer arc current is 100 A, and the non-transfer arc current is 26 A. When the shielding gas flow is 18 L/min, the plasma gas flow is adjusted from 1 to 5 L/min. Similarly, when the plasma gas flow is 3.5 L/min, the shielding gas flow is adjusted from 6 to 30 L/min.

The results show that as the plasma gas flow increases, the maximum arc ignition height first increases sharply and then increases gently. With the increase of shielding gas flow, the maximum arc ignition height first sharply increases and then slowly decreases. During the adjustment of shielding gas flow, a phenomenon was observed where arc noise decreases as the maximum arc ignition height increases.

Reynolds numbers (*Re*) for plasma gas and shielding gas were calculated using Formula (3).

$$Re=\frac{\rho v d}{\eta} \tag{3}$$

Where *Re* is the Reynolds number, ρ is the fluid density, *v* is the fluid velocity, *d* is the characteristic length, and η is the dynamic viscosity coefficient of the fluid.

In this experiment, ρ = 1.7837 (kg/m^3), η = 0.0000202 (Pa·s), d_1 = 0.004 m when calculating plasma gas, and d_2 = 0.012 m when calculating shielding gas. d_1 and d_2 represent the aperture of the conductive nozzle and the shielding gas nozzle, respectively. The fluid velocity (*v*) can be calculated using Formula (4).

$$v = \frac{Q}{\pi(\frac{d}{2})^2} \tag{4}$$

Where Q is the gas flow.

When the *Re* is less than 2300, the fluid is in a laminar state. When the value is between 2300 and 4000, it is in a transitional state; when it exceeds 4000, it is in a turbulent state. The *Re* is 2342.29 when the maximum plasma gas flow is 5 L/min, so it can be roughly considered that the plasma gas has always been in laminar flow during adjustment. The *Re* of the shielding gas flow is 2342.29 at 15 L/min and 4059.96 at 26 L/min, and the flow state is illustrated in Fig. 3. Compared to a turbulent state, a laminar state is considered to have less noise because less air is drawn by the arc, and the noise level is inversely proportional to the arc length. The gas flow parameters of the follow-up experiments were properly selected to ensure the laminar arc, with the shielding gas flow at 18 L/min and the plasma gas flow at 3.5 L/min.

3.1.2 Transfer/non-transfer arc current

The influence of transfer/non-transfer arc current on maximum arc ignition height was studied, as shown in Fig. 4. When the transfer arc current is 100 A, the non-transfer arc current is adjusted from 10 to 150 A. Similarly, when the non-transfer arc current is 26 A, the transfer arc current is adjusted from 50 to 250 A.

The results show that the maximum arc ignition height increases with the non-transfer arc current, but it does not show a significant change with the increase of transfer arc current.

With the increase of non-transfer arc current and transfer arc current, the number of electrons excited by the tungsten electrode will rise. These electrons will collide with plasma gas, ionizing more plasma, consequently increasing the ionization degree in the arc column area [14]. The difference is that the non-transfer arc is generated between the tungsten electrode and the conductive nozzle, and the plasma excited between them can establish a conductive channel between the tungsten electrode and the workpiece. The transfer arc is generated between the tungsten electrode and the workpiece, and it can ignite with the workpiece along the conductive channel. Therefore, the non-transfer arc current plays a decisive role in the arc ignition height, while the transfer arc current can be seen as supplementing plasma for the arc.

The control of arc ignition height by non-transfer arc current can help the arc adapt to various welding conditions. For instance, when the welding torch is too large to fit into narrow gaps, adjusting the arc ignition height can enable the arc to reach the welding location directly.

3.2 Arc shape parameters

3.2.1 Transfer arc current

The influence of transfer arc current on arc shape parameters was studied, as shown in Fig. 5. Among them, the fixed non-transfer arc current is 26 A, and the arc ignition height is 40 mm. The transfer arc current is adjusted from 80 to 250 A, and pictures are taken every 10 A.

The phenomenon depicted in the figure confirms the above analysis. As the

transfer arc current increases, the ionization degree and plasma density in the arc column area also increase, leading to an expansion in the ionization zone profile and the brightness of the arc.

According to Fig. 5(b), as the transfer arc current increases, the expansion speed of the arc bottom is significantly faster than that of the arc root. This may be due to the physical constraint of the arc root by the plasma gas nozzle, similar to how the upper end of water flow is constrained by the water pipe when the faucet is turned on. Therefore, an arc shape with a narrow top and a wide bottom is formed. This arc shape is particularly well-suited for narrow gap welding. Research [15] shows that the bottom corner of the sidewalls is prone to poor fusion during narrow gap welding. The arc expanding at the bottom will provide good coverage for the bottom corner of the sidewalls.

3.2.2 Arc ignition height

The influence of arc ignition height on arc shape parameters was studied, as shown in Fig. 6. Among them, the fixed non-transfer arc current is 26 A, and the transfer arc current is 100 A. The arc ignition height is adjusted from 3 to 36 mm, and pictures are taken every 3 mm.

With the increase of arc ignition height, the arc area undoubtedly increases steadily, the arc projection diameter and arc root diameter change little, and arc brightness decreases. The arc root diameter can be considered to fluctuate around 5 mm, with a variation range of less than 11.2%. However, the arc projection diameter initially increases and then decreases.

When the arc ignition height is short, the arc is constrained by the conductive nozzle, resulting in minimal heat loss of the arc to the surrounding air and concentrated arc energy [16]. As the arc ignition height increases, the restraint effect weakens. Within a certain arc ignition height range, the heat generated by the arc still significantly exceeds heat dissipation, causing the arc to expand. Beyond this range of arc ignition height, the heat loss of the arc increases, leading to a decrease in temperature and an increase in resistance. This causes the arc voltage to increase, the actual arc current to decrease, and the degree of arc ionization to weaken, resulting in arc contraction. It can be inferred that if the arc ignition height continues to increase, the degree of arc contraction will increase until the arc is extinguished.

3.3 Arc pressure

3.3.1 Transfer/non-transfer arc current

The influence of transfer/non-transfer arc current on arc pressure was studied, as shown in Fig. 7. The fixed arc ignition height is 16 mm. When the non-transfer arc current is 26 A, the transfer arc current is adjusted to 100, 150, 200, and 250 A. Similarly, when the transfer arc current is 100 A, the non-transfer arc current is adjusted to 20, 50, 80, and 110 A.

Arc pressure increases significantly with the increase of transfer arc current. When the current is 200 A, the arc pressure is 8 times that of ordinary DC TIG arc pressure (0.11 KPa) [17], which can fully meet the welding requirements. Arc pressure reflects the impact effect of plasma on the molten pool [18], so welding formation can be adjusted by the transfer arc current.

3.3.2 Arc ignition height

The influence of arc ignition height on arc pressure is studied, as shown in Fig. 8. The fixed non-transfer arc current is 26 A, and the transfer arc current is 100 A. During the experiment, the tungsten electrode was directed at the guide hole on the arc pressure tester. The arc pressure was recorded after the arc was ignited and the value stabilized. The arc ignition height was adjusted from 2 to 44 mm, and the arc pressure data were collected every 2 mm.

With the increase of arc ignition height, the arc pressure initially decreases sharply and then decreases slowly. The arc pressure at 20 mm has been reduced to 0.16 KPa, which is equivalent to the arc pressure (0.15 KPa) of a 100A ordinary DC TIG. This confirms the above analysis. As the arc ignition height increases, the degree of arc ionization decreases, leading to a decrease in the number of plasma, which in turn reduces the impact on the molten pool. Therefore, to ensure a good welding formation effect, the proper arc ignition height should be adjusted when the current is fixed. Similarly, the proper transfer arc current should be adjusted when the arc ignition height is fixed.

3.4 Welding application prospect

A novel idea would be to apply laminar plasma arc to narrow gap welding. Compared with the traditional narrow gap arc welding process, it offers two unique advantages:

(1) Improving welding efficiency. Traditional narrow gap arc welding processes have a short arc ignition height (≤4 mm). Therefore, it is necessary to extend the welding torch into the narrow gap groove when welding thick plates. The large size of the welding torch increases the gap size, requiring more welding wire to fill it, thus decreasing welding efficiency [19]. While some solutions, like lengthening the electrode, extending it into the groove [20, 21], and using a sheet tungsten electrode [22], have been proposed, they have resulted in decreased welding quality, increased process complexity, and higher costs. The ignition height of the laminar plasma arc can reach 60 mm. When welding thick plates, there is no need to extend the welding torch into the groove; only extending the arc to the bottom of the groove is required. This approach eliminates the impact of the welding torch size on the gap size, thereby enhancing welding efficiency.

(2) Improve the poor sidewall fusion. The traditional narrow gap arc welding process has poor coverage of the sidewall bottom corner because the energy is concentrated at the bottom of the arc, the arc ignition height is short, and the welding torch flexibility is limited [23]. Although solutions such as bending the electrode [24] and magnetically controlled oscillating arc [25] have appeared, they have increased costs and process complexity. The arc bottom of the laminar plasma arc is very wide, allowing it to effectively cover the bottom corner of the sidewall. A comparison of advantages is shown in Fig. 9 (a) and (b).

However, due to the principle of minimum voltage, the arc should first ignite with the sidewall of the workpiece closest to the tungsten electrode and cannot reach the bottom of the workpiece, as shown in Fig. 9(c). Combined with the above experiments, 304 stainless steel with dimensions of 100×80×20 mm was actually

welded using the welding parameters shown in Table 1. The gap width is 10 mm, the groove depth is 15 mm, and the wire material is 308 stainless steel. The arc shape is shown in Fig. 9(d). It is shown that the arc does not ignite with the sidewall but directly reaches the bottom of the groove. This phenomenon can be attributed to the ignition mechanism of the laminar plasma arc. The laminar non-transfer arc has a long arc ignition height and extends to the bottom of the groove along the axis of the tungsten electrode, as shown in Fig. 9(e). The laminar non-transfer arc acts as a conductive channel between the tungsten electrode and the bottom of the groove, and the transfer arc will ignite at the bottom of the groove along this conductive channel, satisfying the principle of minimum voltage, as shown in Fig. 9(f).

The relative height between the welding torch and the specimen was fixed, and the specimen was welded in a single pass with four layers. The arc shape of each layer and the welding formation are shown in Fig. 10. The results show that the arc has good stability. The welding formation is excellent, showing an inverted triangular shape, and no sidewall unfused defects were found.

4 Conclusions

(1) The non-transfer arc current is positively related to the arc ignition height. It is also positively related to the arc pressure, but the influence is extremely weak. In this experiment, the maximum arc ignition height can reach 60 mm, which is significantly greater than that achieved in the conventional plasma arc welding process.

(2) The transfer arc current is positively related to arc size and brightness, and also positively related to arc pressure. When the transfer arc current is 250 A, the non-transfer arc current is 26 A, and the arc ignition height is 16 mm, the arc pressure can reach 1.87 KPa.

(3) The arc ignition height is negatively related to arc brightness and arc pressure. The arc pressure sharply decreases with the increase of arc ignition height below 20 mm.

(4) The transfer arc plays a major role in welding formation, while the non-transfer arc can enhance welding adaptability by controlling the arc ignition height.

(5) Compared with the traditional narrow gap arc welding process, laminar plasma arc narrow gap welding does not require a welding torch to extend into the groove. The arc provides good coverage on the bottom corner of the sidewall, enhancing welding efficiency and quality.

(6) Under suitable welding parameters, the laminar plasma arc narrow gap welding process is stable. It produces an inverted triangle welding morphology, and no sidewall unfused defects are found.

Ethical Approval

We comply with the COPE guidelines and make the following commitments. All the data and experimental contents involved in this manuscript are original. It does not involve publishing in any form or language elsewhere. The quoted words of other people are marked in the text by reference.

Consent to Participate

All co-authors are aware of the writing and publication of this article and agree to publish it.

Consent to Publish

All co-authors agree to publish this article.

Funding

The present research work was financially supported by Shenyang Collaborative Innovation Center Project for Multiple Energy Fields Composite Processing of Special Materials (Grant No. JG210027) and Shenyang Key Lab of High-tech Welding Power Source and Equipment (Grant No. S220058) and the National Natural Science Foundation of China (Grant No. 52175428)

Competing Interests

The authors declare that they have no known competing financial interests or personal relationships that could have appeared to influence the work reported in this paper.

Availability of data and materials

All data in this manuscript is original and does not involve any copyright issues.

Authors' contributions

Honglei Zhao: Conceptualization, Methodology, Writing-original draft. **Siyu Zhang:** Collecting documents, Writing-original draft. **Xianglong Yu:** Conceptualization, Collecting documents, Writing-original draft. **Yiwen Li:** Collecting documents, Supervision. **Junyan Miao:** Collecting documents, Supervision. **Chenhe Chang:** Writing-review & editing, Resources. **Yunlong Chang:** Project administration, Supervision.

Acknowledgements

The present research work was financially supported by Shenyang Collaborative Innovation Center Project for Multiple Energy Fields Composite Processing of Special Materials (Grant No. JG210027) and Shenyang Key Lab of High-tech Welding Power Source and Equipment (Grant No. S220058) and the National Natural Science Foundation of China (Grant No. 52175428)

References

[1] Pragatheswaran, T., Rajakumar, S., and Balasubramanian, V. "Influence of plasma gas flow rate on the mechanical and microstructural aspects of plasma arc welded titanium alloy joints", *JME,* **17**(3), pp. 080-086 (2022). https://doi.org/10.37255/jme.v17i3pp080-086

[2] Li, M., Lu, T., Dai, J., et al. "Microstructure and mechanical properties of 308L stainless steel fabricated by laminar plasma additive manufacturing", *Mat. Sci. Eng. A-Struct*, **770**, pp. 138523 (2020). https://doi.org/10.1016/j.msea.2019.138523

[3] Cai, D., Luo, Z., Han, S., et al. "Plasma characteristics of a novel coaxial laser-plasma hybrid welding of Ti alloy", *Opt. Laser Eng.*, **167**, pp. 107599 (2023). https://doi.org/10.1016/j.optlaseng.2023.107599

[4] Zhang, H.Y., Mauer, G., Liu, S., et al. "Modeling of the effect of carrier gas injection on the laminarity of the plasma jet generated by a cascaded spray gun", *Coatings*, **12**(10), pp. 1416 (2022). https://0-doi-org.brum.beds.ac.uk/10.3390/coatings12101416

[5] Zhang, H.Y., Li, C.X., Liu, S.H., et al. "Splash involved deposition behavior and erosion mechanism of long laminar plasma sprayed NiCrBSi coatings", *Surf. Coat. Tech.*, **395**, pp. 125939 (2020). https://doi.org/10.1016/j.surfcoat.2020.125939

[6] Liu, S.H., Zhang, S.L., Li, C.X., et al. "Generation of long laminar plasma jets: Experimental and numerical analyses", *Plasma Chem. Plasma P.*, **39**, pp. 377-394 (2019). https://doi.org/10.1007/s11090-018-9949-4

[7] Kruchinin, A.M., Pogrebisskiy, M.Y., Ryazanova, E.S., et al. "Conditions for plasma jet formation in a laminar plasmatron", *Inorganic Materials: Applied Research*, **10**, pp. 572-577 (2019). https://doi.org/10.1134/S2075113319030195

[8] Zhang, F., Pan, G.W., Zhao, Y.H., et al. "Development and application of a cutting and dismantling device for nuclear facility decommissioning based on laminar flow plasma", *Nuclear Fusion and Plasma Physics*, **43**(02), pp. 145-149 (2023). https://doi.org/10.16568/j.0254-6086.202302004

[9] Guo, D., Yu, D., Zhang, P., et al. "Laminar plasma jet surface hardening of the U75V rail steel: Insight into the hardening mechanism and control scheme", *Surf. Coat. Tech.*, **394**, pp. 125857 (2020). https://doi.org/10.1016/j.surfcoat.2020.125857

[10] Samion, M.F.I., Norizat, N.Z., and Mokhtar, A.R.A. "Flow study in structure of the plasma torch for microwave plasma spray", *J. Mod. Manuf. Syst. Technol.*, **4**(2), pp. 56-60 (2020). https://doi.org/10.15282/jmmst.v4i2.5251

[11] Li, M., Lu, T., Dai, J., et al. "Microstructure and mechanical properties of 308L stainless steel fabricated by laminar plasma additive manufacturing", *Mat. Sci. Eng. A-Struct*, **770**, pp. 138523 (2020). https://doi.org/10.1016/j.msea.2019.138523

[12] Liu, Q., Zeng, L., Luo, D.Y., et al. "Reserch on the application of laminar plasma in welding", *Electr. Weld. Mach.*, **48**(10), pp. 17-20 (2018). https://doi.org/10.7512/j.issn.1001-2303.2018.10.04

[13] Zhao, H.L., Zhang, S.Y., Yu, X.L., et al. "Study on arc behavior and weld formation of magnetically controlled narrow gap tig welding", *Int. J. Precis. Eng. Man.*, **26**(3), pp. 651-662 (2025). https://doi.org/10.1007/s12541-024-01140-2

[14] Xu, R.Q., and Chen, M.H. "Identification of ionization region profile and potential distribution in welding arc plasma by direct probe detection", *IEEE T. Plasma Sci.*, **51**(7), pp. 2004-2009 (2023). https://doi.org/10.1109/TPS.2023.3282986

[15] Sun, Q., Liu, Y.B., Qian, X.J., et al. “The wetting and stirring behavior of molten pool in narrow gap AMF-GTAW by numerical and experi-mental analysis”, *J. Mater. Res. Technol.*, **26**, pp. 4835-4847 (2023). https://doi.org/10.1016/J.JMRT.2023.08.184

[16] Fan, C.L., Chen, C., Lin, S.B., et al. “Effect of welding parameters on holographic interferometric fringe in TIG”, *Hanjie Xuebao,* **41**(2), pp. 1-5 (2020). https://doi.org/10.12073/j.hjxb.20190115004

[17] Dong, Z.H., Li, Y.W., Wu, H., et al. “Effect of TIG arc characteristics on weld morphology and structure of AISI444 ferritic stainless steel under pulse current”, *Weld. World,* **65**, pp. 2093-2104 (2021). https://doi.org/10.1007/s40194-021-01168-2

[18] Li, T.Q., Yang, X.M., Chen, L., et al. “Arc behaviour and weld formation in gas focusing plasma arc welding”, *Sci. Technol. Weld. Joi.*, **25**(4), pp. 329-335 (2020). https://doi.org/10.1080/13621718.2019.1702284

[19] Zhao, H.L., Zhang, S.Y., Yu, X.L., et al. “Research status of insufficient sidewalls penetration in narrow gap TIG welding of thick metal plates”, *Int. J. Adv. Manuf. Tech.*, **134**, pp. 39-56 (2024). https://doi.org/10.1007/s00170-024-14204-4

[20] Liu, G., Tang, X., Han, S., et al. “Influence of interwire angle on undercutting formation and arc behavior in pulsed tandem narrow-gap GMAW”. *Mater. Design*, **193**, pp. 108795 (2020). https://doi.org/10.1016/j.matdes.2020.108795

[21] Huang, J., Chen, H., He, J., et al. “Narrow gap applications of swing TIG-MIG hybrid weldings”, *Journal Mater. Process Tech.*, **271**, pp. 609-614 (2019). https://doi.org/10.1016/j.jmatprotec.2019.04.043

[22] Li, Y.B., Ma, S.C., and Ye, T. “Numerical simulation study on correlation between characteristics of slice tungsten electrode pulsed arc with insulating wall constrain and transverse shrinkage deformation of groove in ultra-narrow gap”, *Int. J. Adv. Manuf. Tech.*, **127**(11-12), pp. 5755-5774 (2023). https://doi.org/10.1007/s00170-023-11989-8

[23] Zhao, H.L., Zhang, S.Y., Chen, H., et al. “Methods to improve TIG welding efficiency”, *T. Indian I. Metals*, **77**, pp. 2231-2245 (2024). https://doi.org/10.1007/s12666-024-03323-x

[24] Su, N., Wang, J.Y., Xu, G.X., et al. “Infrared visual sensing detection of groove width for swing arc narrow gap welding”, *Sensors*, **22**(7), pp. 2555 (2022) . https://doi.org/10.3390/s22072555

[25] Jian, X.X., and Wu, H.B. “Influence of the longitudinal magnetic field on the formation of the bead in narrow gap gas tungsten arc welding”. *Metals*, **10**(10), pp. 1351 (2020). https://doi.org/10.3390/met10101351

List of Captions

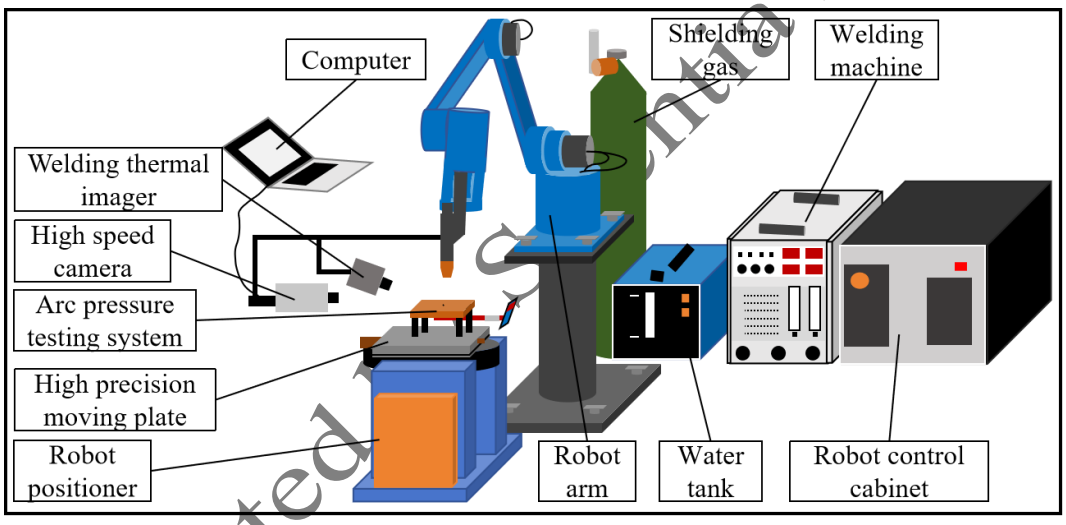

Fig. 1 Experimental platform

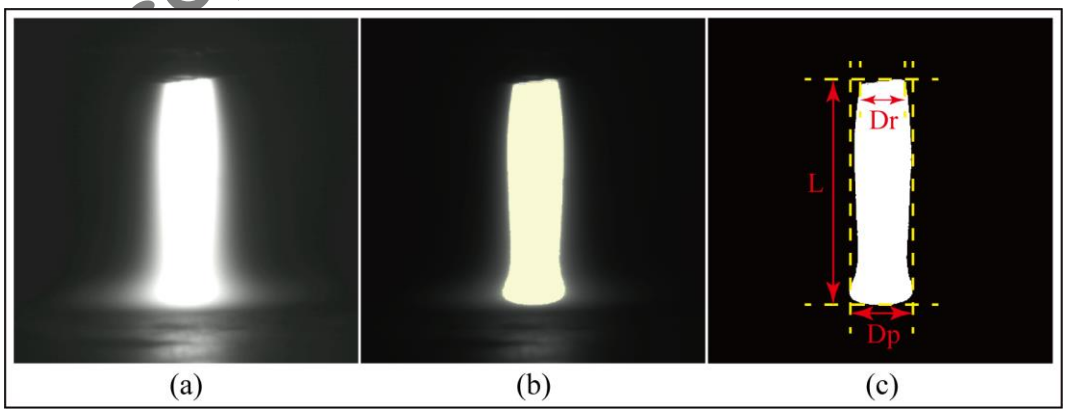

Fig. 2 Arc shape processing

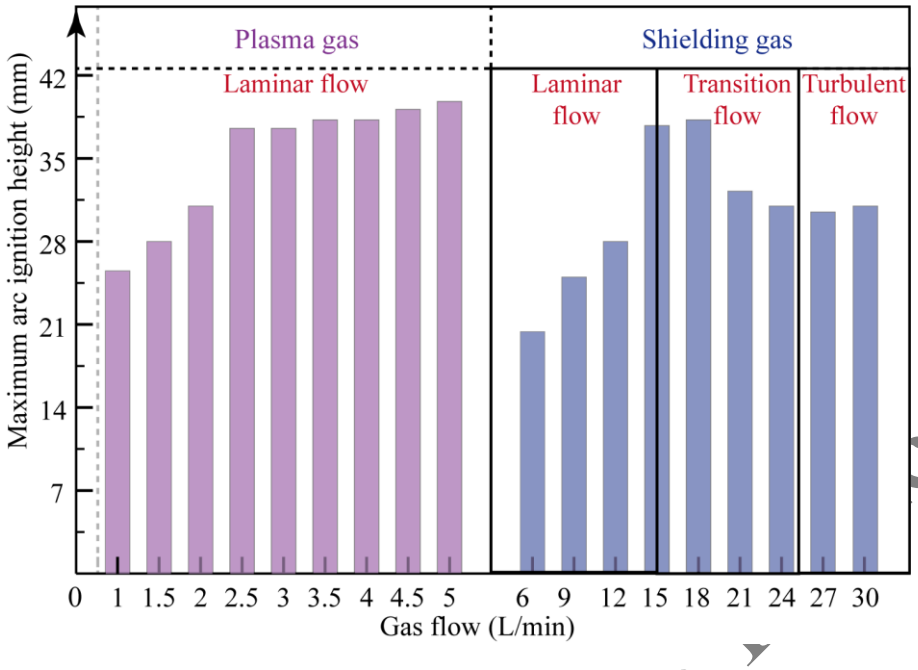

Fig. 3 Influence of shielding/plasma gas flow on maximum arc ignition height

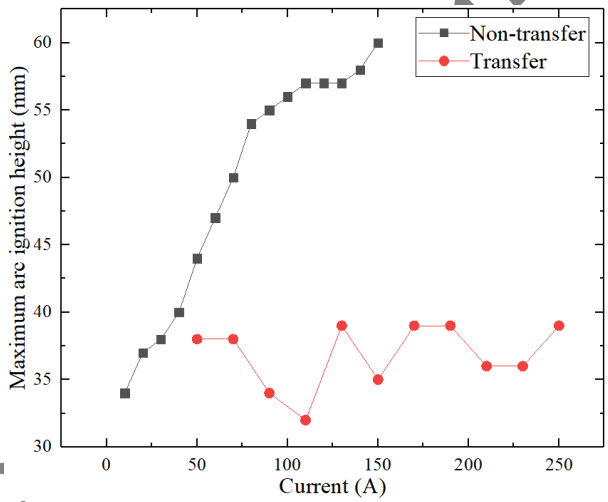

Fig. 4 Influence of transfer/non-transfer arc current on maximum arc ignition height

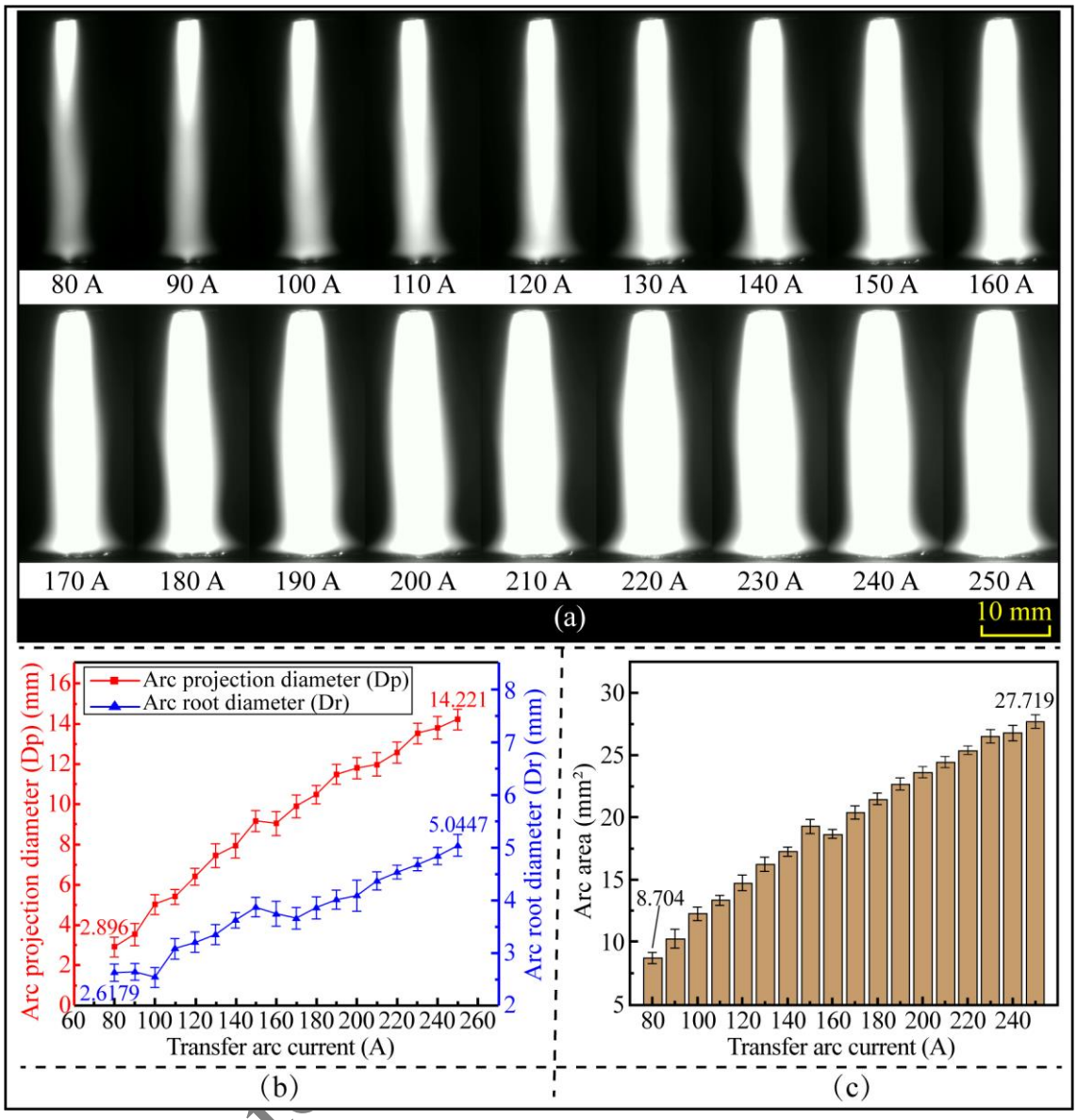

Fig. 5 Influence of transfer arc current on arc shape parameters
(a) Arc shape (b) Arc projection diameter and arc root diameter (c) Arc area

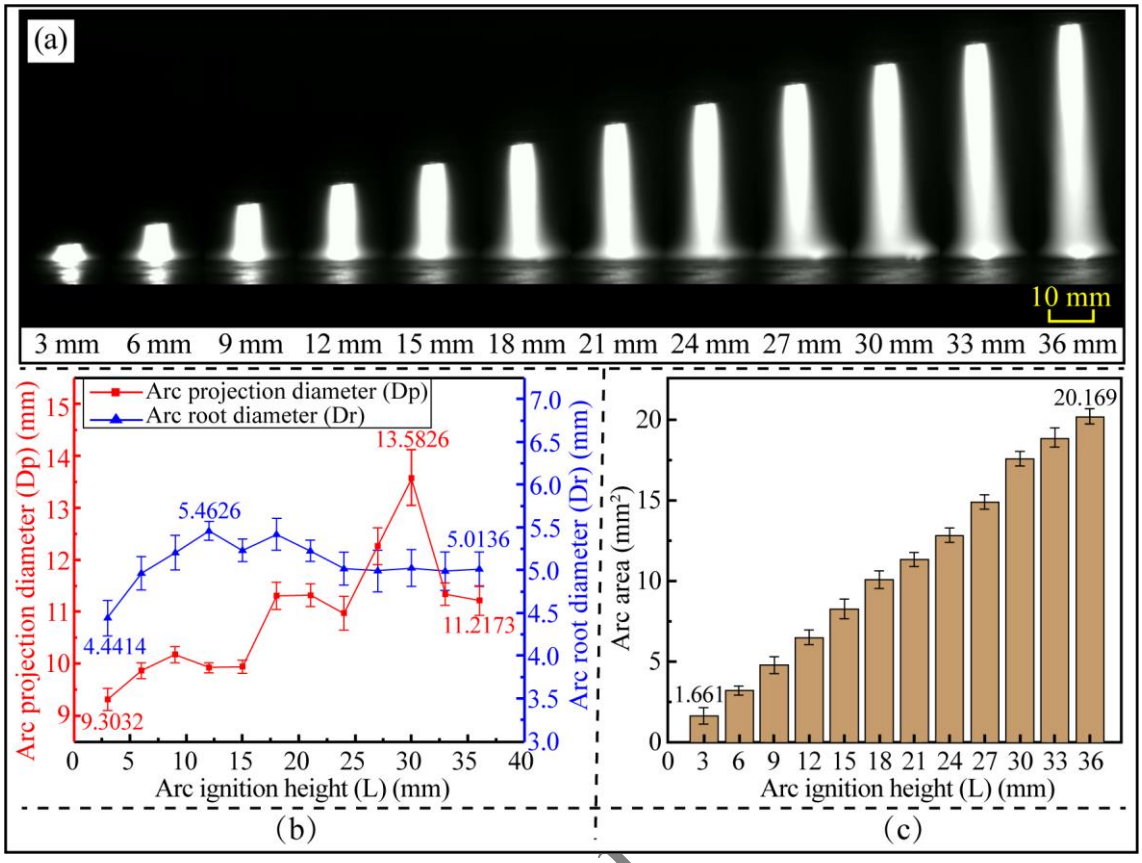

Fig. 6 Influence of arc ignition height on arc shape parameters

(a) Arc shape (b) Arc projection diameter and arc root diameter (c) Arc area

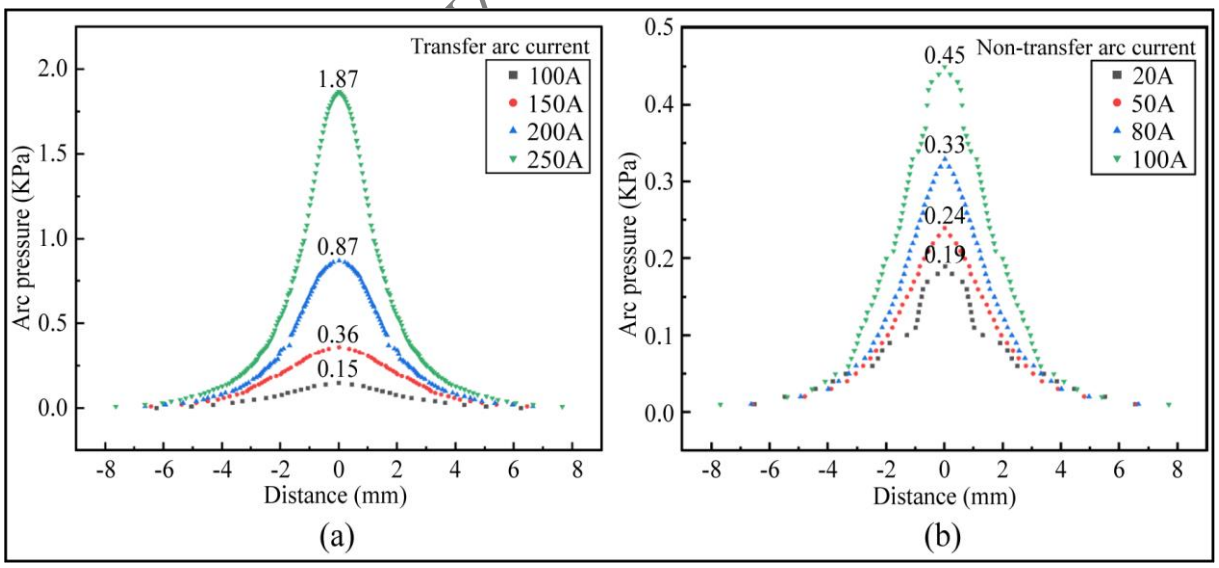

Fig. 7 Influence of transfer/non-transfer arc current on arc pressure

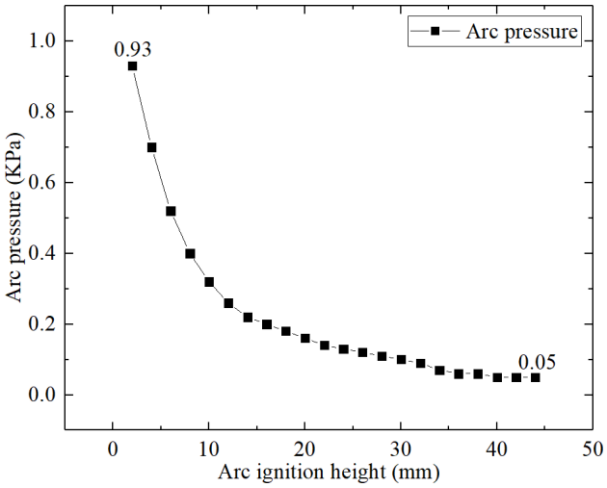

Fig. 8 Influence of arc ignition height on arc pressure

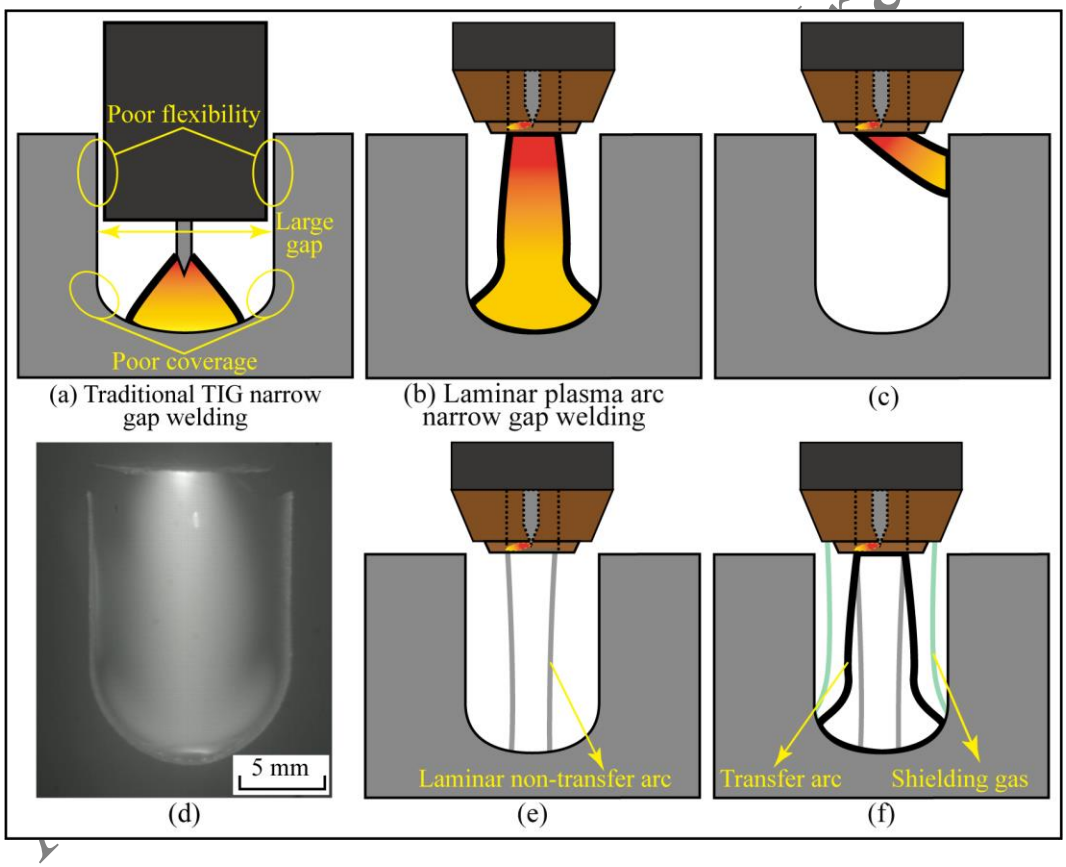

Fig. 9 Laminar plasma arc narrow gap welding

Table 1 Welding parameters

Transfer arc current (A)	Non-transfer arc current (A)	Welding speed (mm/s)	Argon flow (L/min)	Plasma gas flow (L/min)	Wire feeding speed (m/min)	Arc ignition height (mm)
250	26	1	18	3.5	1.8	16

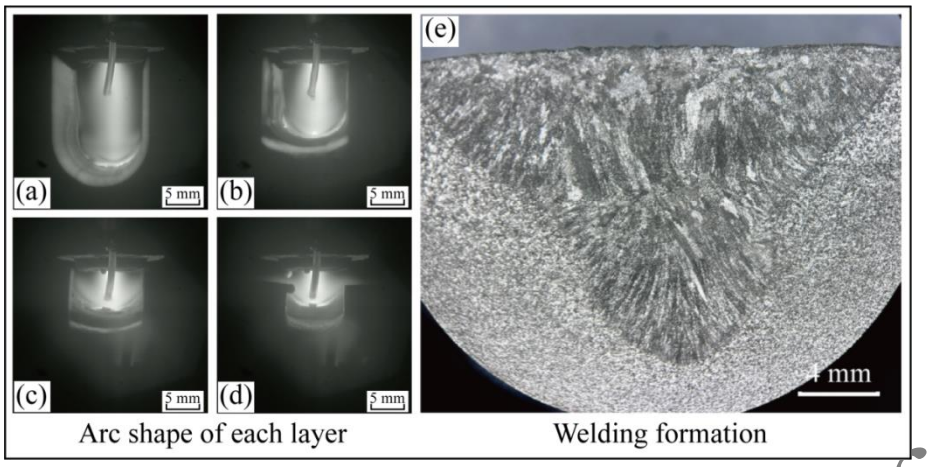

Fig. 10 Arc shape of each layer and welding formation

Biographies

Honglei Zhao is currently a PhD student at the School of Materials Science and Engineering, Shenyang University of Technology. In this school, he obtained a bachelor's degree in welding technology and engineering in 2019 and a master's degree in material engineering in 2022. His research interests are new technologies and ideas for high-efficiency and high-quality welding, focusing on narrow gap welding and wire arc additive manufacturing.

Siyu Zhang is currently a PhD student at the School of Materials Science and Engineering, Shenyang University of Technology. In this school, he obtained a bachelor's degree in material forming and control engineering in 2010 and a master's degree in material engineering in 2017. He is a senior engineer in welding and has been engaged in welding technology and the design of large compressors for 10 years. His research focuses on welding technology and automatic control.

Xianglong Yu is currently a master's student at the School of Materials Science and Engineering, Shenyang University of Technology. His research focuses on welding technology and equipment.

Yiwen Li is currently a PhD student at the School of Materials Science and Engineering, Shenyang University of Technology. In this school, he obtained a bachelor's degree in welding technology and engineering in 2019 and a master's degree in materials science and engineering in 2021. His research focuses on magnetically controlled arc and welding equipment.

Junyan Miao is currently a PhD student at the School of Materials Science and Engineering, Shenyang University of Technology. He obtained a bachelor's degree in welding technology and engineering and a master's degree in materials science and engineering from Jiangsu University of Science and Technology in 2019 and 2021, respectively. His research focuses on numerical simulation of welding arc and welding process design.

Chenhe Chang works at Liaoning Xinyuan Special Welding Technology Co., Ltd. He has been engaged in welding structures and welding inspection for 5 years.

Yunlong Chang obtained a bachelor's degree and a master's degree in welding technology and equipment from Shenyang University of Technology in 1987 and 1993, respectively. In 1998, he obtained a PhD in welding technology and equipment from South China University of Technology. He is currently a professor at Shenyang University of Technology. His research interests are multi-physical field coupling welding equipment technology and application, and efficient intelligent welding technology.